Peer-reviewed version available at *Biomolecules* **2018**, *8*, 32; doi:10.3390/biom8020032

# FMSP-Nanoparticles induced cell death on human breast adenocarcinoma cell line (MCF-7 cells): Morphometric Analysis

**Firdos Alam Khan ***

Department of Stem Cell Biology, Institute for Research and Medical Consultations, Imam Abdulrahman Bin Faisal University, Post Box No. 1982, Dammam 31441, Saudi Arabia

Electronic address: fakhan@iau.edu.sa

**Sultan Akhtar**

Department of Biophysics, Institute for Research and Medical Consultations, Imam Abdulrahman Bin Faisal University, Post Box No. 1982, Dammam 31441, Saudi Arabia

Electronic address: suakhtar@iau.edu.sa

**Sarah Ameen Almofty**

Department of Stem Cell Biology, Institute for Research and Medical Consultations, Imam Abdulrahman Bin Faisal University, Post Box No. 1982, Dammam 31441, Saudi Arabia

Electronic address: saalmofty@iau.edu.sa

**Dana Almohazey**

Department of Stem Cell Biology, Institute for Research and Medical Consultations, Imam Abdulrahman Bin Faisal University, Post Box No. 1982, Dammam 31441, Saudi Arabia

Electronic address: daaalmohazey@iau.edu.sa

**Munthar Alomari**

Department of Stem Cell Biology, Institute for Research and Medical Consultations, Imam Abdulrahman Bin Faisal University, Post Box No. 1982, Dammam 31441, Saudi Arabia

Electronic address: maomari@iau.edu.sa

***Corresponding author contact details:**

**Firdos Alam Khan**

Department of Stem Cell Biology, Institute for Research and Medical Consultations,
Imam Abdulrahman Bin Faisal University, Post Box No. 1982,
Dammam 31441,
**Saudi Arabia**

Phone: + 966-1333-30866

Electronic address: fakhan@iau.edu.sa

## ABSTRACT

Breast cancer treatment mostly revolved around radiation therapy and surgical interventions, these treatments doesn't provide satisfactory relief to the patients and carry unmanageable side-effects. Nanomaterials show promising results in treating cancer cells and have many advantages such as high biocompatibility, bioavailability and effective therapeutic capabilities. Interestingly, fluorescent magnetic nanoparticles have been used in many biological and diagnostic applications, but there is no report of use of fluorescent magnetic submicronic polymer nanoparticles (FMSP-nanoparticles) in the treatment of human breast cancer cells. In the present study, we have tested the effect FMSP-nanoparticles on human breast cancer cells (MCF-7). We have tested different concentrations (1.25µg/1mL, 12.5µg/mL and 50µg/1mL) of FMSP-nanoparticles in MCF-7 cells and evaluated the nanoparticles response morphometrically. Our results revealed that FMSP-nanoparticles produced a concentration dependent effect on the cancer cells, dose of 1.25µg/mL produced no significant effect on the cancer cell morphology and cell death, whereas dosages of 12.5µg/mL and 50µg/mL respectively showed significant nuclear augmentation, disintegration, chromatic condensation followed by dose dependent cell death. Our results demonstrate FMSP-nanoparticles have ability to induce cell death in MCF-7

cells and may be considered as a potential anti-cancer agent for breast cancer treatments.

**KEYWORDS**

fluorescent magnetic submicronic polymer nanoparticles, human breast cancer, MCF-7 cell line, anticancer, cytotoxicity, *in vitro* cell culture

## INTRODUCTION

Breast cancer is the most commonly diagnosed cancer in women and one of the major reasons of cancer death among women. Despite improved precautionary, preventive and treatment strategies, there is no complete cure for the cancer (De Hoon et al., 2012; Guarneri et al., 2012). Currently, breast cancer treatment mostly revolved around radiation and surgical interventions, each one of them has its own side-effect issues. Traditionally, the cancer is treated with chemotherapy, hormonal therapy, targeted therapy, and immunotherapy modalities, but all of them carry some side effects and shortcomings (Liu et al., 2009; Li et al., 2012). The reason for these shortcomings and side-effects are mostly due to non-specificity and systemic toxicity of anti-cancer drugs (Guo, et al, 2011; Yokoyama, et al., 2009; Wang, et al., 2011). But the major cause of the failure of current drug therapy, is the high rate of drug resistance of cancer cells (Ozben, et al., 2006). In this background, there is an urgent need of alternative approach towards cancer management and treatments. Over the past few years, nanoparticles have generated tremendous interests in cancer treatments owing to their precise targeting, biocompatibility, bioavailability, and multifunctional capabilities (Afrimzon et al., 2008; Zhao and Castranova, 2011; Aftab et al., 2018).

Based on the chemical compositions, nanoparticles can be broadly classified into two major classes like organic materials which are liposomes, dendrimers, carbon nanotubes, emulsions, and other polymers, and inorganic materials which include metals (Chowdhury, et al., 2016; Chowdhury, et al., 2016; Kuang, et al., 2009). In the recent past, several attempts have been made to study the effect of different classes of nanoparticles on cancer cells (Pati et al., 2016; Yaffee et al., 2015; Wang et al., 2014; Mathew et al., 2011; Rasmussen et al., 2010; Wang et al., 2009; Turcotte et al., 2008; Hanley C, et al., 2008; Unfried et al., 2007; Smalley & Herlyn, 2006; Wood et al., 2005; Gottlieb et al., 2003). Interestingly, fluorescent magnetic nanoparticles have been used in a wide range of applications in biological systems such as diagnostic, bioimaging, and drug delivery (Pei et al., 2018; Jha et al., 2017; Long et al., 2017; Gupta et al. 2016; Narayanan et al., 2012; Gupta et al., 2012; Gupta et al., 2011; Padhya et al., 2015; Gao et al., 2009; Chan et al., 1998; Larson et al. 2003; Dam et al., 2012; Xu et al., 2018; Kaewsaneha et al., 2014; Long et al., 2013; Grafton et al., 2011; Govindaiah et al., 2010; Bollhorst et al., 2003; Huang et al., 2002) and also in detection of foodborne pathogens (Bruno et al., 2017), but there is no report of use of fluorescent magnetic submicronic polymer nanoparticles (FMSP-nanoparticles) in the treatment of human breast cancer cells. the present study, we have tested the effect FMSP-nanoparticles on human breast cancer cells (MCF-7). We have used different concentrations of FMSP-nanoparticles and evaluated their cytotoxic effects by morphometric analysis after 6hrs and 24hrs post-treatments.

## MATERIALS & METHODS

### Synthesis and Characterization of FMSP-nanoparticles

FMSP-nanoparticles were obtained from Professor Hamid Abdelhamid Eliassari, University of Lyon, F-69622 Lyon, France. The method of synthesis and characterization of FMSP-nanoparticles has been described in detail in a paper published by Lansalot et al., 2005. Detail procedure is described below:

**Materials:** Deionized water (Millipore Milli-Q purification system) was used in the entire study. Magnetic emulsions and film-forming nanoparticles (Rhodopas Ultrafine PR 3500) were provided by Ademtech SA (Pessac,France) and Rhodia (Aubervilliers, France), respectively. The fluorescent nanoparticles (FluoSpheres F-8787) were purchased from Molecular Probes, polyethyleneimine (PEI,Mw=25,000 g/mole), purchased from Aldrich and a modified polyacrylic acid-based amphiphilic graft copolymer (Coatex M883, Mw=50,000 g/mol, 21 weight%) ; critical aggregation concentration=1.4 g/L at pH9) were provided by Coatex, Lyon, France. The main features of the oil-in water magnetic emulsions are listed in Table 1.

**Table 1: Features of magnetic emulsions used:**

| **Reference** | **ME1** | **ME2** |
|---|---|---|
| $D_h$(nm)[a] | 246 | 249 |
| $D_n$(nm)[b] | 219 | 221 |
| $D_w$(nm)[b] | 233 | 232 |
| Polydispersity index[b] | 1.066 | 1.050 |
| Solid content (%) | 6.1 | 9.7 |
| Density (g $cm^{-3}$) | 2.66 | 2.42 |
| Magnetic content (wt%) | 70 | 70 |

[a]Obtained from Dynamic Light Scattering (DLS)

Preprints (www.preprints.org) | NOT PEER-REVIEWED | Posted: 15 May 2018 doi:10.20944/preprints201805.0204.v1

Peer-reviewed version available at Biomolecules 2018, 8, 32; doi:10.3390/biom8020032

[b]Obtained from TEM analysis

The chemical composition and colloidal characterization was done as per method described by Montagne et al. 2012. The synthesis can be briefly described as follows: an organic ferrofluid composed of iron oxide nanoparticles stabilized in octane by a surrounding oleic acid layer, was emulsified in water with non-ionic surfactants (nonylphenol ether (NP10) and t-octylphenoxypolyethoxyethanol (Triton X-405)). Table 2 displays the characteristics of the film forming and fluorescent nanoparticles.

**Table 2: Features of film-forming and fluorescent nanoparticles used:**

| **Reference** | **Rhodopas PR 3500** | **Yellow-green fluospheres** |
|---|---|---|
| $D_h$(nm)[a] | 47 | 24 |
| Polymer nature | Acrylic copolymer ($T_g \sim 10^0$C)[b] | Polystyren ($T_g \sim 10^0$C)[c] |
| Density (g cm$^{-3}$) | 1.03[d] | 1.04c |
| Fluorescence | / | $\lambda_{exc}$ = 505 nm[c] $_{em}$= 515 nm[c] |

[a] Obtained from Dynamic Light Scattering (DLS)

[b] Obtained from Differential Scanning Calorimetry

[c] Reference

[d] As per Rhodia

**Preparation of the cationic magnetic emulsion:** Preparation of the cationic magnetic emulsion: Two millilitre of deionized water were added to either 2 ml

(ME1) or 1.2 ml (ME2) of the anionic magnetic emulsion and the mixture was homogenized by vortex mixing. After magnetic separation, the supernatant was removed, and the magnetic droplets were then dispersed in 4 ml of water. Following a further step of homogenization and magnetic separation, 2 ml of water was added. After redispersion, this 2 ml of washed magnetic emulsion was added to 4 ml of a PEI solution. After 15 min of stirring, the magnetic droplets were washed two times using 4 ml of water, before finally redispersion in 2 ml of water.

**Polyethyleneimine adsorption study:** The amount of PEI adsorbed onto the magnetic droplets was deduced by titrating the free PEI via specific amine titration using fluorescamine. The fluorescent product obtained was quantified using a fluorescence spectrophotometer (LS 50 system, Perkin Elmer). A calibration curve was first established (emission intensity measured at 472 nm for an excitation wavelength of 388 nm). The procedure was as follows: PEI standard solutions in milli-Q grade water were prepared, ranging from 0.1 mg mL)1 to 1 mg mL)1. Standard solution of volume 100 lL was added to 2.9 mL of 0.01 Mborate buffer pH 9.1, then 1 mL of 0.3 mg mL)1 fluorescamine solution in acetone was also added. The PEI amino groups and fluorescamine were then allowed to react for 24 h in the dark. ME1 was used for this study, with all the quantities adjusted to use low volumes (100 lL) rather than 2 mL. The concentration of PEI solutions ranged from C0=0.1 to 25 mg mL)1 for a pH between 8 and 11 depending on PEI concentration. After the PEI adsorption step, 100 lL of supernatant was withdrawn and allowed to react with fluorescamine.

**Hetero-coagulation step:** The film-forming nanoparticles and 10 M NaCl were placed in a 100 mL thermostat reactor. The pH was first adjusted to 7.0 with 1 M HCl. The cationic magnetic emulsion (2 mL) obtained in the former stage was mixed with

12 mL of 10 M NaCl (pH 7.0), and continuously added 20 mL to the reactor content. The temperature was set at $20^0$ Celsius during the hetero-coagulation process.

**Film-formation step:** Magnetic hetero-coagulates (magnetic emulsion droplets surrounded by polymer nanoparticles) were separated from the supernatant via magnetic separation and then dispersed in a solution of the amphiphilic copolymer Coatex M883 (0.8 g L)1 of 0.01 M borate buffer solution). After a second magnetic separation, the hetero-coagulates were re-dispersed in Coatex M883 solution, then placed in the reactor heated at $50^0$Ceslius (temperature above the Tg of the film-forming nanoparticles) and stirred for 20 hrs.

**Characterization of FMSP-nanoparticles:** The structure and morphology of FMSP-nanoparticles was examined by scanning electron microscopy (SEM) (FEI, INSPECT S50, Check Republic), and the size of fluorescent submicron magnetic nanoparticle was measured by transmission electron microscopy (TEM) (FEI, MORGAGNE.68, Check Republic) respectively. This TEM and SEM analysis was done at Department of Biophysics, Institute for Research and Medical Consultations, Imam Abdulrahman Bin Faisal University, Dammam, Saudi Arabia.

**Treatment of FMSP-nanoparticles**

MCF-7 is a breast cancer cell line isolated in 1970 from a 69-year-old Caucasian woman is well characterized cancer cell line. The MCF-7 cell line was obtained from Dr Khaldoon M. Alsamman, Clinical Laboratory Science, College of Applied Medical Science, Imam Abdulrahman Bin Faisal University, Dammam, Saudi Arabia. MCF-7 cells were cultured in T25 flask containing the DMEM media containing L-glutamine, 10% FBS, selenium chloride, 120 U/ml penicillin, and 120 µg/ml streptomycin at 37°Celsius in 5% CO2 incubator (Heracell 150i, Thermoscientific). The cells were then seeded into 96-well cell culture plates to be used for FMSP-

nanoparticles treatments. The cells with more than 80% confluence were used for FMSP-nanoparticles treatment and before treatments, FMSP-nanoparticles was autoclaved for 30 min to remove the contaminations. The cancer cells were treated with different concentrations of FMSP-nanoparticles (1.25µg/mL, 12.5µg/mL, and 50µg/mL) and cells were observed after 6hrs and 24hrs intervals. To obtain an accurate statistical calculation, triplicate samples were considered for both control and treated groups.

**Morphometric Analysis:**

At the end of each treatment (6hrs and 24hrs), the cells treated with different concentrations of FMSP-nanoparticles were removed from the $CO_2$ incubator and were observed under an inverted microscope (TS100F Eclipse, Nikon) equipped with a digital camera. We have used 10X, 20X and 40X magnifications to examine the anatomy and structure of both treated and control cells.

**DAPI Staining:**

The DAPI staining assay was carried out to examine the effect of nanoparticles on cell nucleus. Both control and treated cells were pre-treated with the freshly prepared ice-cold (4%) paraformaldehyde. The cells were treated with 0.1% Triton X-100 in PBS for 5 min for permeabilization of cell membranes. After that cells were stained with DAPI with concentration 1 µg/mL prepared in PBS for 5 min in the dark environment. Thereafter, the cells were washed with 0.1% Triton X-100 prepared in PBS. The cell morphology was analysed by laser confocal microscope (Zeiss, Germany) equipped with a digital camera. The difference between live cells and dead cells were calculated and compared in both control and FMSP-nanoparticles treated groups respectively.

**Statistical analysis:**

All data were presented as mean ± standard deviation from triplicate experiments. Statistical analysis was performed using ANOVA followed by Dunnett's post hoc test of GraphPad Prism software. * $P < 0.05$, and ** $P < 0.01$ were considered statistically significant.

## RESULTS

### Characterization of FMSP-nanoparticles

The morphology, structure and size of FMSP-nanoparticles was determined by using SEM and TEM investigations. SEM analysis showed that nanoparticles were crystallized, and spherical in shape (Figure 1); whereas TEM analysis revealed nanoparticles have an average diameter of 100 to 400 nm (Figure 2).

### Morphology of the FMSP-nanoparticles treated MCF-7 cells

Both control and FMSP-nanoparticles-treated cells were observed under 100X, 200X and 400X magnifications to study detailed morphological changes. The dose of 1.25µg/mL produced no cell death when observed under 100X magnification (Figures 3a-c), when observed under 400X magnification we also did not see any morphological changes as compared to control cells (Figures 4a-c). We did not find any difference in cells morphology and structure in both 6hrs and 24hrs post-treatments respectively.

When MCF-7 cells were treated with dose of 12.5µg/mL, 6 hrs post-treatment showed moderate morphological changes in cell morphology and structure observed under 100X magnification (Figure 5b) as compared to control group's cells (Figure 5a). When cells were observed 24hrs post-treatment, we saw cell death in major part of the

culture plate (Figures 5c, 6c). Under 400x magnification, we saw dead cells and their debris and cells with nuclear augmentation (Figure 6c).

MCF-7 cells were treated with dose of 50µg/mL, 6 hrs post-treatment showed significant morphological changes in cell structure and numbers (Figure 7b) as compared to control group's cells (Figure 7a). After 24hrs post-treatment, cells were observed under 400X magnification, we could see extensive damage in cellular structure and contents of the nanoparticles-treated cells (Figure 7c). We also found many dead cells and their debris (Figure 8c) with compared to control group of cells (Figure 8a). In addition, nanoparticle-treated cells also showed significant nuclear condensation and nuclear fragmentation (Figures 8b, 8c).

**Cell death analysis by DAPI Staining**

During morphological analysis, we could see lots of cell death, especially with 12.5µg/mL and 50µg/mL treated cells. With a view to confirm the cell death due to apoptosis pathway, we had stained cells with DAPI. DAPI staining was done to evaluate the effect of FMSP-nanoparticles on cell nucleus of both control and treated cells. DAPI staining was carried out with 1.25µg/mL, 12.5µg/mL and 50µg/mL of FMSP-nanoparticles dosages for 24 hrs post-treatment. Treatment with 1.25µg/mL dose showed no nuclear disintegration (Figure 9b) as compared to control cells (Figure 9a), whereas treatment with 12.5µg/mL showed a significant amount of nuclear death (Figure 9a). The dose 50µg/mL dose showed a highly significant amount of nuclear disintegration and cell death (Figure 9d). We have calculated the number of live cells after 24 hrs of FMSP-treatments. When cells were treated with dose 1.25ug/mL, we have found that the cancer cells viability was 92.50% (Figure 10) but when the cells

were treated with 12.5ul/mL and 50ug/mL, the cancer cells showed dose-dependent decreased in the cell viability (39.25% and 60.35%) respectively (Figure 10).

## DISCUSSION

This is the first study in which we have studied in detail the morphological and structural changes caused due to nanoparticle treatments. The morphological analysis with various magnifications (100X, 200X and 400X) of the cells revealed that FMSP-nanoparticles produced a dose-dependent effects on the MCF-7 cells. For example, the dose 1.25µg/mL produced a no effect on the cell morphology, whereas the dosages 12.5µg/mL initiated the cell nucleus augmentation, nucleus fragmentation and cell death. Strikingly, the dose with 50µg/mL showed a strong effect on both cell morphology and cell death. For example, post 6hrs treatment, there was a strong indication of cell death observed as compared to control group cells and clear sign of early nuclear fragmentation. Post 24hrs and 48hrs treatments showed a high degree of chromatin condensation, nuclear condensation and nuclear fragmentation, with strong presence of cellular debris. The present study is first of its kind where FMSP-nanoparticles treated cancer cells were morphologically analysed in detail. Recently, it has been reported that nanoparticles treatment caused cell morphology (Zielinska et al., 2018), but most of the studies by and large are confined to the quantitative aspects of nanoparticles. Our findings demonstrate that it is equally important to do a morphological analysis of the cells-treated with nanoparticles. The morphological analysis provides the information about the extent of nanoparticles effects on cancer cells and their internal organizations. Under high magnification, we could see the extent of nanoparticles impact on cancer cell numbers, nucleus and cell membrane. As most of the cancer cells were found to be dead with dose of 50µg/mL, it would be

interesting to examine the effects of nanoparticles on other cell organelles such as mitochondria, endoplasmic reticulum, Golgi apparatus, and other components of the cells.

Magnetic nanoparticles have excellent characteristics for better target drug delivery (Matthaiou et al., 2014; Barar Jet al., 2014; Heidari et al., 2013; Khosroushahi et al., 2012; Omidi et al., 2011; Moogooee et al., 2011; Mooguee et al., 2010) and effective-way of treating cancer (Heidari et al., 2013). During our morphological analysis, we found that high dose of FMSP-nanoparticles caused cytotoxic effects on MCF-7 cells which lead to nuclear disintegration and fragmentation followed by death. Moreover, a high dosage of FMSP-nanoparticles seems to induce MCF-7 cell death via apoptosis that was demonstrated by results from the DAPI (6-diamidino-2-phenylindole) nuclear staining technique. This staining technique is known to form fluorescent complexes with double strand DNA. The apoptotic nuclei which undergo nuclear fragmentation and chromatin condensation can stain by DAPI (Lin-Wei et al., 2016; Shiva et al., 2015). We have found that the cells treated with 1.25µg/mL dose showed no nuclear disintegration as compared to control group cells. The 12.5µg/mL and 50µg/mL dosages caused a significant nuclear fragmentation, disintegration. The nuclear fragmentation and disintegration are an indication of apoptosis. Similar results are reported where nanoparticles caused nuclear fragmentation, disintegration and cell death in cancer cells (Baharara et al., 2016; Mytych et al.,2015).

During our study, we also measured an average size of the FMSP-nanoparticles to be able to understand how these nanoparticles produced a cytotoxic effect on cancer cells. In our findings, the SEM and TEM analysis revealed that FMSP-nanoparticles

with 100 to 200 mm size caused significant cell death of cancer cells. While we don't know the mechanism of interaction of FMSP-nanoparticles with cancer cells, but the possibility of cell internalization cannot be ruled out. There are several reports of internalization of nanoparticles studied in various cancerous cells (Serpe et al., 2014; Chen et al., 2013; Thomas et al., 2012;) which led to cell death.

## CONCLUSION

The present findings confirmed that FMSP-nanoparticles induced cell death in a dose dependent manner and FMSP-nanoparticles could. DAPI staining confirmed the cell death due to nuclear disintegration, hence the role of apoptosis induced cell death cannot be ruled out. The dose of 1.25µg/mL produced no significant effect on the cell death, whereas those of 12.5µg/mL produced a significant cell death 24hrs post-treatment. The interestingly dose of 50µg/mL caused a highly significant cell death during the same period. We have demonstrated that the FMSP-nanoparticles are potential biomaterials to be used in the treatment of cancer.

## LIST OF ABBREVIATIONS

µg =Microgram

µl =Microliter

$CO_2$= Carbon dioxide

DAPI = 4′,6-diamidino-2-phenylindole

DMEM= Dulbecco's Modified Eagle Medium

DMSO= Dimethyl sulfoxide

FBS = Fetal bovine serum

HCL = Hydrochloric acid

IU = International Unit

FMSP-nanoparticles= Fluorescent magnetic submicronic polymer nanoparticles

M = Molar

MCF-7 = Michigan Cancer Foundation-7

mL=Millilitre

MNPs = Magnetic nanoparticles

NaCL = Sodium Chloride

nm =Nanometre

NPs = Nanoparticles

SEM = Scanning electron microscopy

TEM = Transmission electron microscopy

**ETHICS APPROVAL AND CONSENT TO PARTICIPATE:** Not Applicable

**CONSENT FOR PUBLICATION:** This manuscript is approved by all authors for the submission.

**AVAILABILITY OF DATA AND MATERIAL:** The data analyzed are available from the corresponding author upon a request.

**COMPETING INTERESTS:** The authors declare that they have no competing interests.

**FUNDING:** Financial support received from Deanship of Scientific Research, Imam Abdulrahman Bin Faisal University, Dammam, Saudi Arabia (Grant Number: 2018-004-IMRC).

## ACKNOWLEDGEMENTS

Authors are thankful to the entire management of the Institute for Research & Medical Consultations (IMRC), Imam Abdulrahman Bin Faisal University, Dammam, Saudi Arabia for their support and encouragement. We are thankful to Mr. Dionecio Jr. Bagon Dela Roca for assisting the cell culture and bioassay related work. We are also thankful to Dr. Khaldoon M. Alsamman, Clinical Laboratory Science, College of Applied Medical Science, Imam Abdulrahman Bin Faisal University, Dammam, Saudi Arabia for providing MCF-7 cell line. We also thankful to Professor Abdelhamid Eliassari, University of Lyon, F-69622 Lyon, France, University Lyon 1, Villeurbanne, CNRS, UMR 5007, LAGEP-CPE, 43 Bd. 11 Novembre 1918, F-69622 Villeurbanne, France providing the nanoparticles.

## REFERENCES

1. Afrimzon E, Deutsch A, Shafran Y, Zurgil N, Sandbank J, Pappo I, et al. Intracellular esterase activity in living cells may distinguish between metastatic and tumor-free lymph nodes. Clin. Exp. Metastasis. 2008;25:213–24.
2. Aftab S, Shah A, Nadhman A, Kurbanoglu S, Aysıl Ozkan S, Dionysiou DD, Shukla SS, Aminabhavi TM. Nanomedicine: An effective tool in cancer therapy. Int. J. Pharm. 2018 Feb 7;540(1-2):132-149.
3. Baharara J, Ramezani T, Divsalar,A, Mousavi, M and Seyedarabi A. Induction of Apoptosis by Green Synthesized Gold Nanoparticles Through Activation of

Caspase-3 and 9 in Human Cervical Cancer Cells. Avicenna J Med Biotechnol. 2016 Apr-Jun; 8(2): 75–83.

4. Barar J, Omidi Y. Surface modified multifunctional nanomedicines for simultaneous imaging and therapy of cancer. Bioimpacts. 2014;4:3–14.

5. Bollhorst T, Shahabi S, Wörz K, Petters C, Dringen R, Maas M, Rezwan K.

6. Bruno JG, Sivils JC, Phillips T. Aptamer-Magnetic Bead Quantum Dot Sandwich Assays for Foodborne Pathogen Detection: Pros, Cons, and Lessons Learned. J AOAC Int. 2017 Jul 1;100(4):895-899. doi: 10.5740/jaoacint.17-0163. Epub 2017 Jun 16.

Cain K. Chemical-induced apoptosis: formation of the Apaf-1 apoptosome. Drug. Metab. Rev. 2003; 35:337–63.

7. Chan W. C. W. & Nie S. Quantum Dot Bioconjugates for Ultrasensitive Nonisotopic Detection. Science 281, 2016–2018 (1998).

8. Chen H, Zhang T, Zhou Z, Guan M, Wang J, Liu L, et al. Enhanced uptake and cytotoxity of folate-conjµgated mitoxantrone-loaded micelles via receptor up-regulation by dexamethasone. Int. J. Pharm. 2013; 448:142–9

9. Chowdhury, E.H. *Nanotherapeutics: From Laboratory to Clinic*; CRC Press: Boca Raton, FL, USA, 2016.

10. Chowdhury, E.H.; Rosli, R.; Karim, M.E. Systemic Delivery of Nanoformulations of Anti-Cancer Drugs with Therapeutic Potency in Animal Models of Cancer. *Curr. Cancer Ther. Rev.* 2016, *12*, 1–17.

11. Dam D. H. M. et al. Direct Observation of Nanoparticle–Cancer Cell Nucleus Interactions. ACS Nano 6, 3318–3326 (2012).

12. De Hoon, J.P.; Veeck, J.; Vriens, B.E.; Calon, T.G.; van Engeland, M.; Tjan-Heijnen, V.C. Taxane resistance in breast cancer: A closed HER2 circuit? *Biochim. Biophys. Acta* 2012, *1825*, 197–206.

13. Gao J, Gu H, Xu B. Multifunctional magnetic nanoparticles: design, synthesis, and biomedical applications. Acc Chem Res. 2009 Aug 18;42(8):1097-107.

14. Gottlieb E, Armour SM, Harris MH, Thompson CB. Mitochondrial membrane potential regulates matrix configuration and cytochrome c release during apoptosis. Cell Death Differ. 2003;10(6):709–717.

15. Govindaiah P, Jung YJ, Lee JM, Park TJ, Ryu du Y, Kim JH, Cheong IW. Monodisperse and fluorescent poly(styrene-co-methacrylic acid-co-2-naphthyl methacrylate)/Fe3O4 composite particles. J. Colloid Interface Sci. 2010 Mar 15;343(2):484-90.

16. Grafton MM, Wang L, Vidi PA, Leary J, Lelièvre SA. Breast on-a-chip: mimicry of the channeling system of the breast for development of theranostics. Integr. Biol. (Camb). 2011 Apr;3(4):451-9.

17. Guarneri, V.; Dieci, M.V.; Conte, P. Enhancing intracellular taxane delivery: Current role and perspectives of nanoparticle albumin-bound paclitaxel in the treatment of advanced breast cancer. *Expert Opin. Pharmacother.* 2012, *13*, 395–406.

18. Guo, J.; Bourre, L.; Soden, D.M.; O'Sullivan, G.C.; O'Driscoll, C. Can non-viral technologies knockdown the barriers to siRNA delivery and achieve the next generation of cancer therapeutics? *Biotechnol. Adv.* 2011, *29*, 402–417.

19. Gupta B. K. et al. Highly Luminescent–Paramagnetic Nanophosphor Probes for In Vitro High-Contrast Imaging of Human Breast Cancer Cells. Small 8, 3028–3034 (2012).

20. Gupta B. K. et al. Probing a Bifunctional Luminomagnetic Nanophosphor for Biological Applications: a Photoluminescence and Time-Resolved Spectroscopic Study. Small 7, 1767–1773 (2011).

21. Gupta BK, Singh S, Kumar P, Lee Y, Kedawat G, Narayanan TN, Vithayathil SA, Ge L, Zhan X, Gupta S, Martí AA, Vajtai R, Ajayan PM, Kaipparettu BA. Bifunctional Luminomagnetic Rare-Earth Nanorods for High-Contrast Bioimaging Nanoprobes. Sci Rep. 2016 Sep 2;6:32401.

22. Hanley C, Layne J, Punnoose A, et al. Preferential killing of cancer cells and activated human T cells using ZnO nanoparticles. Nanotech. 2008;19(29):295103.

23. Heidari Majd M, Barar J, Asgari D, Valizadeh H, Rashidi MR, Kafil V, et al. Targeted fluoromagnetic nanoparticles for imaging of breast cancer mcf-7 cells. Adv. Pharm Bull. 2013;3:189–95.

24. Huang H, Dong CY, Kwon HS, Sutin JD, Kamm RD, So PT. Three-dimensional cellular deformation analysis with a two-photon magnetic manipulator workstation. Biophys J. 2002 Apr;82(4):2211-23.

25. Jha DK, Saikia K, Chakrabarti S, Bhattacharya K, Varadarajan KS, Patel AB, Goyary D, Chattopadhyay P, Deb P Direct one-pot synthesis of glutathione capped hydrophilic FePt-CdS nanoprobe for efficient bimodal imaging application. Mater Sci Eng C Mater Biol Appl. 2017 Mar 1;72:415-424.

26. Kaewsaneha C, Bitar A, Tangboriboonrat P, Polpanich D, Elaissari A. Fluorescent-magnetic Janus particles prepared via seed emulsion polymerization. J Colloid Interface Sci. 2014 Jun 15;424:98-103.

27. Khosroushahi AY, Naderi-Manesh H, Yeganeh H, Barar J, Omidi Y. Novel water-soluble polyurethane nanomicelles for cancer chemotherapy:

physicochemical characterization and cellular activities. J Nanobiotechnol. 2012;10:2.

28. Kuang, Y.H.; Chen, X.; Su, J.; Wu, L.S.; Liao, L.Q.; Li, D.; Chen, Z.S.; Kanekura, T. RNA interference targeting the CD147 induces apoptosis of multi-drug resistant cancer cells related to XIAP depletion. *Cancer Lett.* 2009, *276*, 189–195.

29. Lansalot M., M. Sabor., A. Elaissari., C. Pichot. Elaboration of fluorescent and highly magnetic submicronic polymer particles via a stepwise heterocoagulation process. Colloid and Polymer Science. September 2005, Volume 283, Issue 12, pp 1267–1277.

30. Larson D. R. et al. Water-Soluble Quantum Dots for Multiphoton Fluorescence Imaging in Vivo. Science 300, 1434–1436 (2003).

31. Li, J.M.; Wang, Y.Y.; Zhao, M.X.; Tan, C.P.; Li, Y.Q.; Le, X.Y.; Ji, L.N.; Mao, Z.W. Multifunctional QD-based co-delivery of siRNA and doxorubicin to HeLa cells for reversal of multidrug resistance and real-time tracking. *Biomaterials* 2012, *33*, 2780–2790. [

32. Lin-Wei W, Ai-Ping Q, Wen-Lou L, Jia-Mei C, Jing-Ping Yuan, Han Wu, Yan Li, and Juan Liu. Quantum dots-based double imaging combined with organic dye imaging to establish an automatic computerized method for cancer Ki67 measurement. Sci Rep. 2016; 6: 20564.

33. Liu, C.; Zhao, G.; Liu, J.; Ma, N.; Chivukula, P.; Perelman, L.; Okada, K.; Chen, Z.; Gough, D.; Yu, L. Novel biodegradable lipid nano complex for siRNA delivery significantly improving the chemosensitivity of human colon cancer stem cells to paclitaxel. *J. Control. Release* 2009, *140*, 277–283.

34. Long G, Zhang Y, Yang X, Pu J, Qin J, Liu L, Liao F. Facile characterization of the immobilization of streptavidin on magnetic submicron particles with a fluorescent probe of streptavidin. Appl Spectrosc. 2013 Jun;67(6):688-91

35. Long Z, Liu M, Jiang R, Zeng G, Wan Q, Huang H, Deng F, Wan Y, Zhang X2, Wei Y. Ultrasonic-assisted Kabachnik-Fields reaction for rapid fabrication of AIE-active fluorescent organic nanoparticles. Ultrason Sonochem. 2017 Mar;35(Pt A):319-325.

36. Long Z, Liu M, Mao L, Zeng G, Huang Q, Huang H, Deng F, Wan Y, Zhang X, Wei Y.One-step synthesis, self-assembly and bioimaging applications of adenosine triphosphate containing amphiphilies with aggregation-induced emission feature. Mater Sci Eng C Mater Biol Appl. 2017 Apr 1;73:252-256.

37. Mathew R, White E. Autophagy in tumorigenesis and energy metabolism: friend by day, foe by night. Curr. Opin. Genet. Dev. 2011;21(1):113–119.

38. Matthaiou EI, Barar J, Sandaltzopoulos R, Li C, Coukos G, Omidi Y. Shikonin-loaded antibody-armed nanoparticles for targeted therapy of ovarian cancer. Int J. Nanomedicine. 2014;9:1855–70.

39. Montagne A, Gauberti M, Macrez R, Jullienne A, Briens A, Raynaud JS, Louin G, Buisson A, Haelewyn B, Docagne F, Defer G, Vivien D, Maubert E. Ultra-sensitive molecular MRI of cerebrovascular cell activation enables early detection of chronic central nervous system disorders. Neuroimage. 2012 Nov 1;63(2):760-70.

40. Moogooee M, Ramezanzadeh H, Jasoori S, Omidi Y, Davaran S. Synthesis and in vitro studies of cross-linked hydrogel nanoparticles containing amoxicillin. J. Pharm Sci. 2011;100:1057–66.

41. Mytych J, Lewinska A, Zebrowski J, Wnuk M. Gold nanoparticles promote oxidant-mediated activation of NF-κB and 53BP1 recruitment-based adaptive response in human astrocytes. Biomed Res Int 2015; 2015: 304575.

42. Narayanan T. N. et al. Hybrid 2D Nanomaterials as Dual-Mode Contrast Agents in Cellular Imaging. Adv. Mater. 24, 2992–2998 (2012).

43. National Cancer Institute at National Institutes of Health (NIH), Cancer Stat Facts: Ovarian Cancer, https://seer.cancer.gov/statfacts/html/ovary.html (2016).

44. Omidi Y. Smart multifunctional theranostics: simultaneous diagnosis and therapy of cancer. Bioimpacts. 2011;1:145–7.

45. Ozben, T. Mechanisms and strategies to overcome multiple drug resistance in cancer. *FEBS Lett.* 2006, *580*, 2903–2909.

46. Padhye P., Alam A., Ghorai S., Chattopadhyay S. & Poddar P. Doxorubicin-Conjugated β-NaYF4:Gd3+/Tb3+ Multifunctional, Phosphor Nanorods: a Multi-Modal, Luminescent, Magnetic Probe for Simultaneous Optical and Magnetic Resonance Imaging and an Excellent pH-Triggered Anti-Cancer Drug Delivery Nanovehicle. Nanoscale, 7, 19501–19518 (2015).

47. Pati R, Das I, Mehta RK, Sahu R, Sonawane A. Zinc-oxide nanoparticles exhibit genotoxic, clastogenic, cytotoxic and actin depolymerization effects by inducing oxidative stress responses in macrophages and adult mice. Toxicol Sci. 2016;150(2):454–472.

48. Pei X, Yin H, Lai T, Zhang J, Liu F, Xu X, Li N. Multiplexed Detection of Attomoles of Nucleic Acids Using Fluorescent Nanoparticle Counting Platform. Anal Chem. 2018 Jan 16;90(2):1376-1383.

49. Rasmussen JW, Martinez E, Louka P, Wingett DG. Zinc oxide nanoparticles for selective destruction of tumor cells and potential for drµg delivery applications. Expert Opin Drug Del. 2010;7(9):1063–1077.

50. Serpe L, Gallicchio M, Canaparo R, Dosio F. Targeted treatment of folate receptor-positive platinum-resistant ovarian cancer and companion diagnostics, with specific focus on vintafolide and etarfolatide. Pharmgenomics Pers Med. 2014;7:31–42.

51. Shiva I, Zhohreh S, Seyed Mohammad A, and Shahriar M. Induction of growth arrest in colorectal cancer cells by cold plasma and gold nanoparticles. Arch Med Sci. 2015 Dec 10; 11(6): 1286–1295.

52. Smalley KS, Herlyn M. Towards the targeted therapy of melanoma. Mini Rev Med Chem. 2006;6(4):387–393.

53. Smoluchowski, M. Drei Vorträge über Diffusion, Brownsche Molekularbewegung und Koagulation von Kolloidteilchen. Physik. Z. (in German). 1916; 17: 557–571, 585–599.

54. Thomas TP, Huang B, Choi SK, Silpe JE, Kotlyar A, Desai AM, et al. Polyvalent dendrimer-methotrexate as a folate receptor-targeted cancer therapeutic. Mol. Pharm. 2012; 9:2669–76.

55. Turcotte S, Chan DA, Sutphin PD, Hay MP, Denny WA, Giaccia AJ. A molecule targeting VHL-deficient renal cell carcinoma that induces autophagy. Cancer Cell. 2008;14(1):90–102.

56. Unfried K, Albrecht C, Klotz LO, von Mikecz A, Grether-Beck S, Schins RPF. Cellular responses to nanoparticles: target structures and mechanisms. Nanotoxicology. 2007;1(1):52–71.

57. Wang H, Wick RL, Xing B. Toxicity of nanoparticulate and bulk ZnO, Al2O3 and TiO2 to the nematode Caenorhabditis elegans. Environ Pollut. 2009;157(4):1171–1177.

58. Wang X, Wang W, Li L, Perry G, Lee HG, Zhu X. Oxidative stress and mitochondrial dysfunction in Alzheimer's disease. Biochim. Biophys. Acta. 2014;1842(8):1240–1247.

59. Wang, Z.; Senzer, D.D.R.; Nemunaitis, J. RNA interference and cancer therapy. *Pharm. Res.* 2011, *28*, 2983–2995.

60. Wood A, Schneider J, Shilatifard A. Cross-talking histones: implications for the regulation of gene expression and DNA repair. Biochem Cell Biol. 2005;83(4):460–467.

61. Xu G, Yan Q, Lv X, Zhu Y, Xin K, Shi B, Wang R, Chen J, Gao W, Shi P, Fan C, Zhao C, Tian H. Visualization of Colorectal Cancers Using Activatable Nanoprobes with Second Near-Infrared Emissions. Angew. Chem. Int. Ed. Engl. 2018 Feb 2.

62. Yaffee P, Osipov A, Tan C, Tuli R, Hendifar A. Review of systemic therapies for locally advanced and metastatic rectal cancer. J Gastrointest Oncol. 2015;6:185–200.

63. Yokoyama, T.; Kondo, Y.; Bögler, O.; Kondo, S. The Role of Autophagy and Apoptosis in the Drug Resistance of Cancer. In *Drug Resistance in Cancer Cells*; Springer: New York, NY, USA, 2009; pp. 53–71.

64. Zhang MZ, Yu Y, Yu RN, Wan M, Zhang RY, Zhao YD. Tracking the down-regulation of folate receptor-alpha in cancer cells through target specific delivery of quantum dots coupled with antisense oligonucleotide and targeted peptide. Small. 2013;9:4183–93.

65. Zhao J, Castranova V. Toxicology of nanomaterials used in nanomedicine. J Toxicol. Environ Health B Crit Rev. 2011;14(8):593–632.

66. Zielinska, E., Zauszkiewicz-Pawlak,A., Wojcik,M and Inkielewicz-Stepniak, I. Silver nanoparticles of different sizes induce a mixed type of programmed cell death in human pancreatic ductal adenocarcinoma. Oncotarget. 2018 Jan 12; 9(4): 4675–4697.

## Figure 1

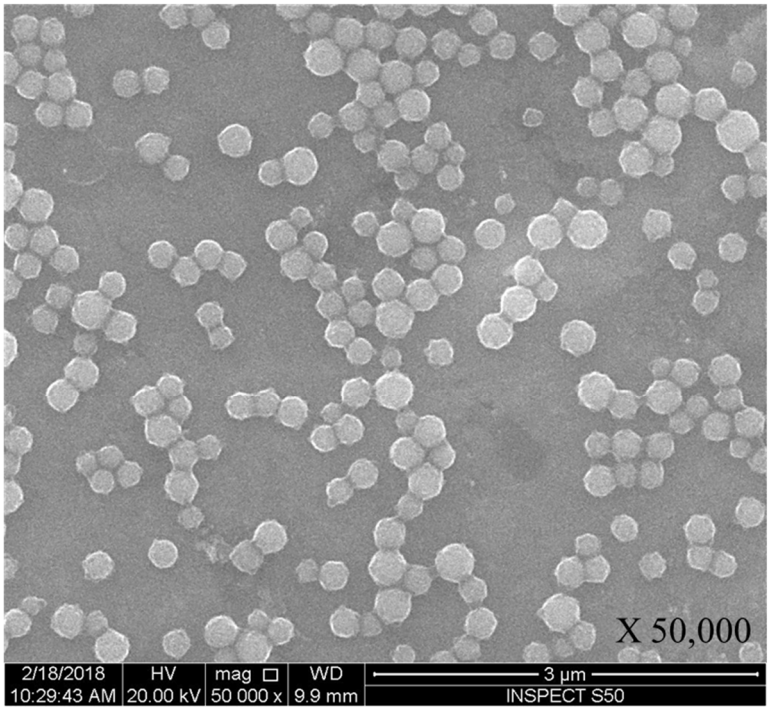


Spherical structure of FMSP-nanoparticles showing through scanning electron microscopy (SEM) with 50,000X magnification.

## Figures 2 a-b

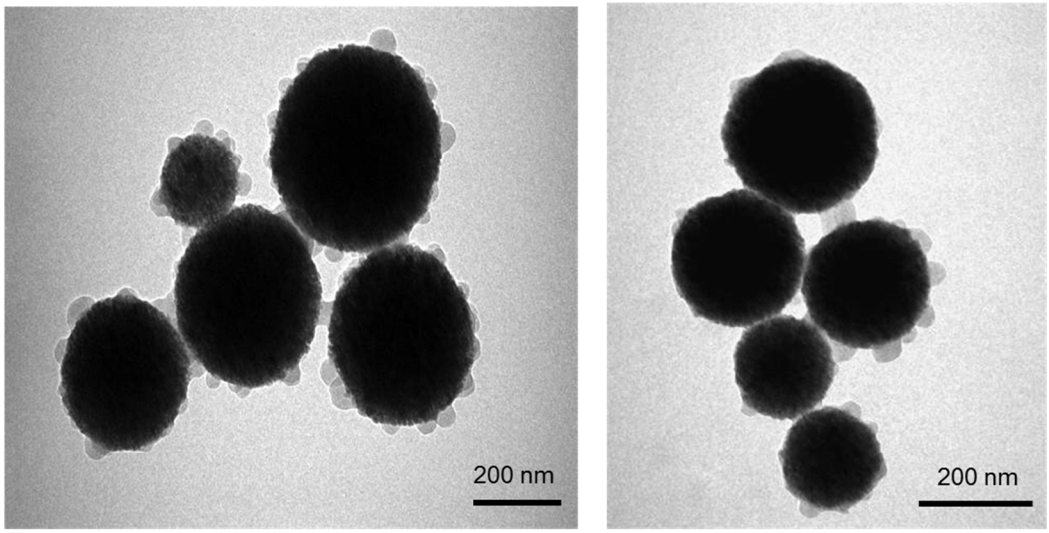


Structure of FMSP-nanoparticles through transmission electron microscopy (TEM) showing spherical shaped nanoparticles with size ranging from 150 nm to 400 nm

## Figures 3a-c

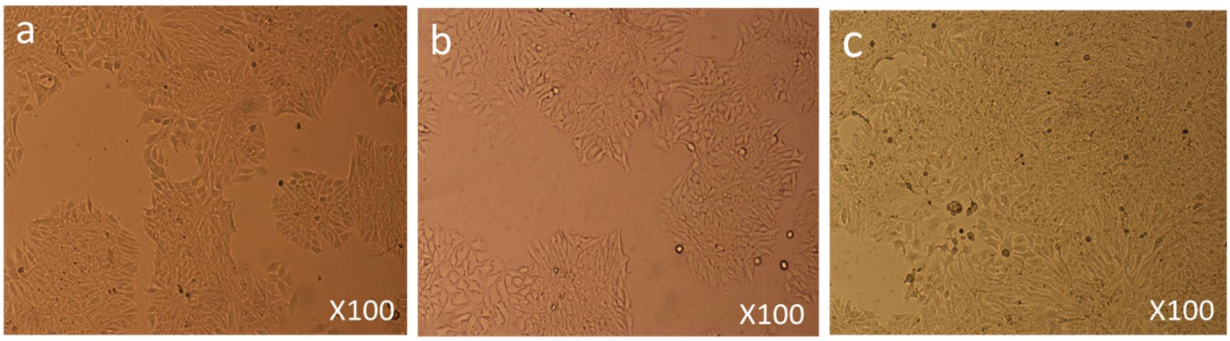


Cell Morphology: The MCF-7 cells showing morphology (a) Control (nontreated) (b) treated with FMSP-nanoparticles (1.25 µg/mL) for 6hrs (c) treated with FMSP-nanoparticles (1.25 µg/mL) for 24 hrs: FMSP-nanoparticles-treated cells not showing any morphological changes with compared to control group cells. 100 X magnification

## Figures 4a-c

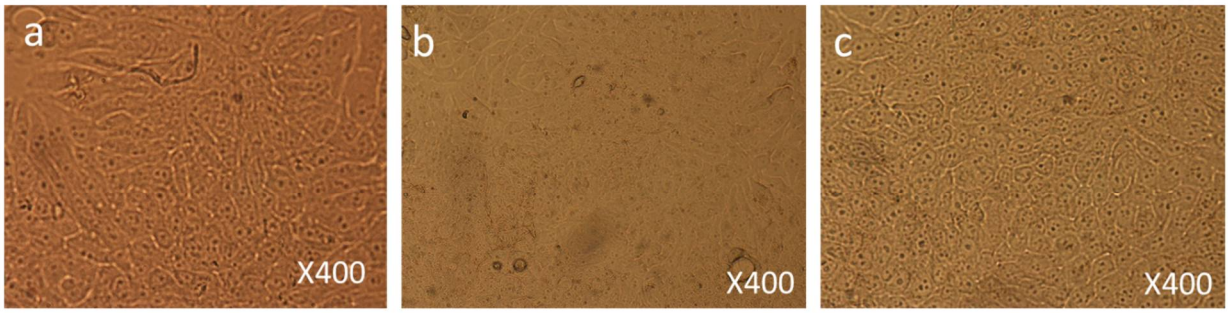


Cell Morphology: The MCF-7 cells showing morphology (a) Control (nontreated) (b) treated with FMSP-nanoparticles (1.25 µg/mL) for 6hrs (c) treated with FMSP-nanoparticles (1.25 µg/mL) for 24 hrs: FMSP-nanoparticles-treated cells not showing any morphological changes with compared to control group cells. 400 X magnification

## Figures 5a-c

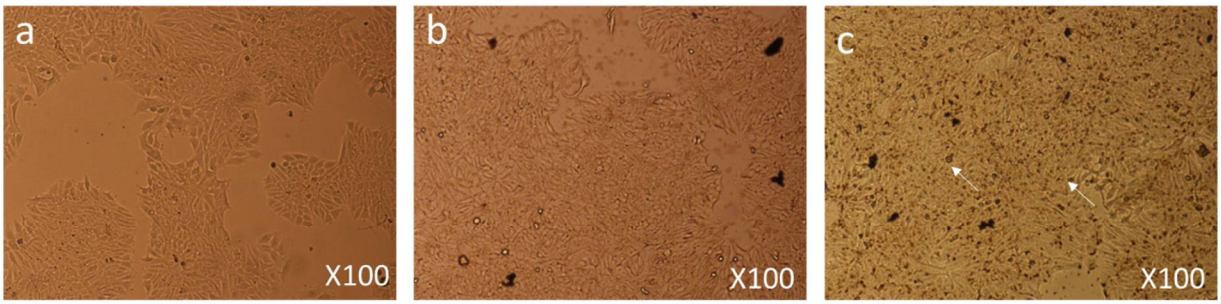


Cell Morphology: The MCF-7 cells showing morphology (a) Control (nontreated) (b) treated with FMSP-nanoparticles (12.5 µg/mL) for 6hrs (c) treated with FMSP-nanoparticles (12.5 µg/mL) for 24 hrs: FMSP-nanoparticles-treated cells showing cell death (arrows) after 24hrs of post-FMSP-nanoparticles treatment. 100 X magnification

## Figures 6a-c

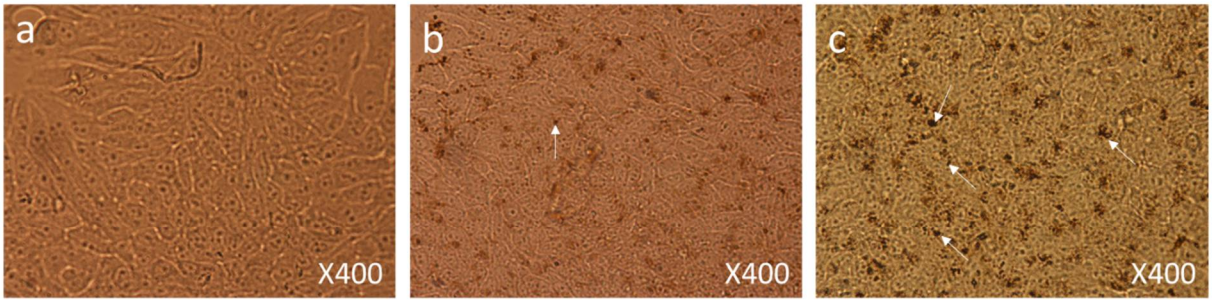


Cell Morphology: The MCF-7 cells showing morphology (a) Control (nontreated) (b) treated with FMSP-nanoparticles (12.5 µg/mL) for 6hrs showing beginning of cell death (arrows) (c) treated with FMSP-nanoparticles (12.5 µg/mL) for 24 hrs: FMSP-nanoparticles-treated cells showing high level of cell death (arrows) after 24hrs of post-FMSP-nanoparticles treatment. 400 X magnification

## Figures 7a-c

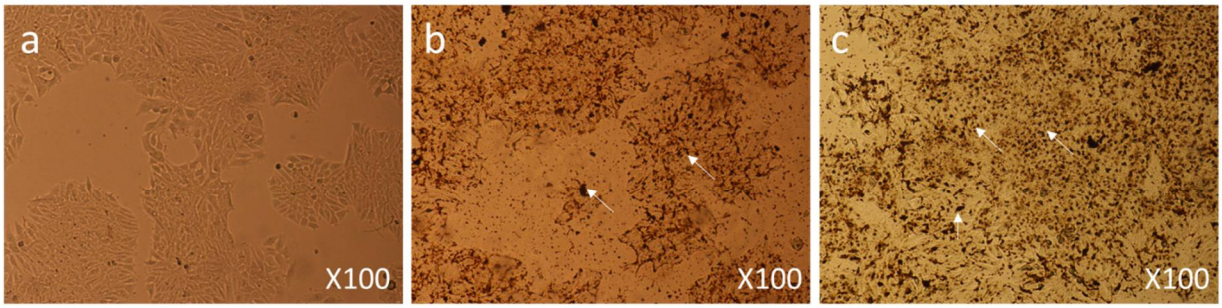


Cell Morphology: The MCF-7 cells showing morphology (a) Control (nontreated) (b) treated with FMSP-nanoparticles (12.5 µg/mL) for 6hrs showing high level of cell death (arrows) (c) treated with FMSP-nanoparticles (12.5 µg/mL) for 24 hrs showing drastic increase in the cell death (arrows) after 24hrs of post-FMSP-nanoparticles treatment. 100 X magnification

## Figures 8a-c

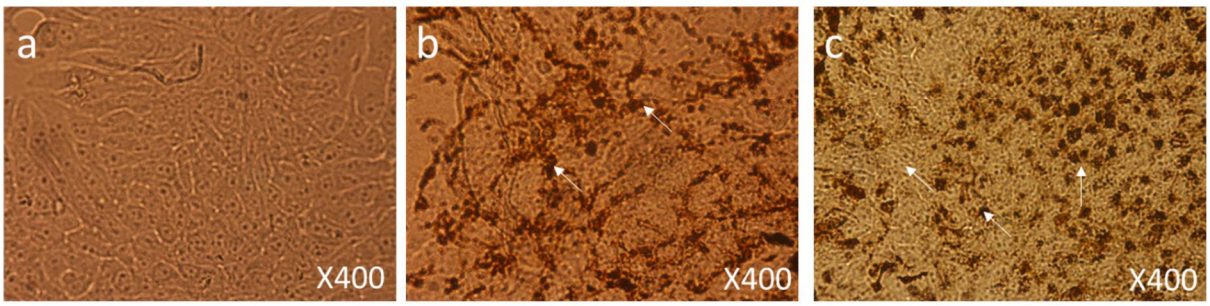


Cell Morphology: The MCF-7 cells showing morphology (a) Control (nontreated) (b) treated with FMSP-nanoparticles (12.5 µg/mL) for 6hrs showing high level of cell death, nuclear disintegration, nuclear augmentation (arrows) (c) treated with FMSP-nanoparticles (12.5 µg/mL) for 24 hrs showing drastic increase in the cell death, nuclear disintegration, nuclear augmentation (arrows) after 24hrs of post-FMSP-nanoparticles treatment. 400 X magnification

## Figure 9a-d

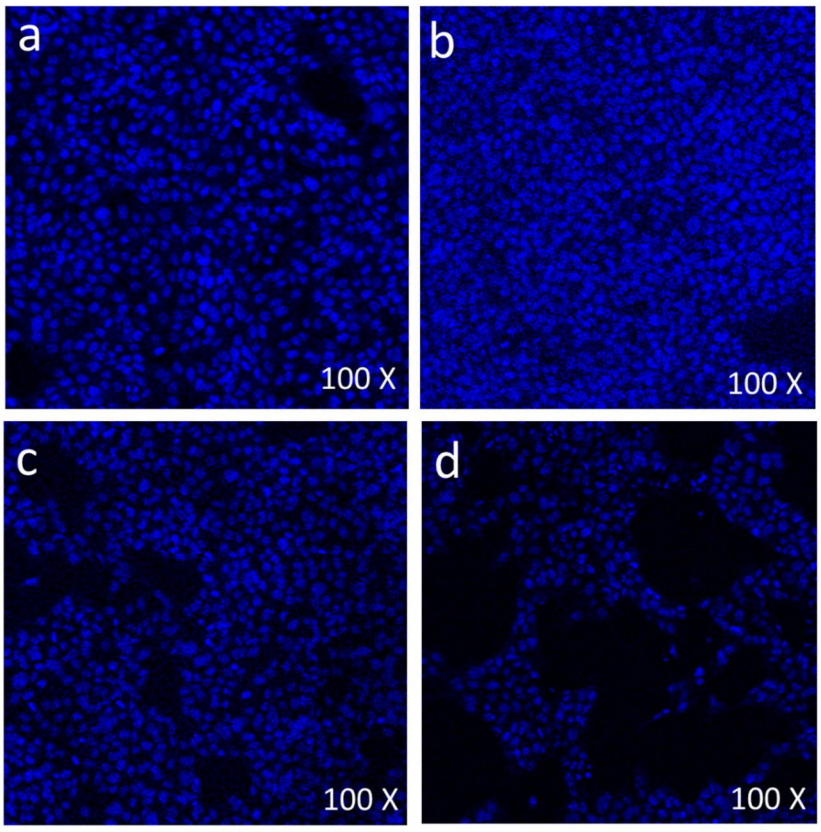


Scanning confocal microscopic images of MCF-7 cells stained with DAPI (blue color): The control cells (without FMSP-nanoparticles treatment) (a) and with FMSP-nanoparticles (1.25 µg/mL) (b), 12.5ug/mL (c) and 50ug/mL (d)

**Figure 10**

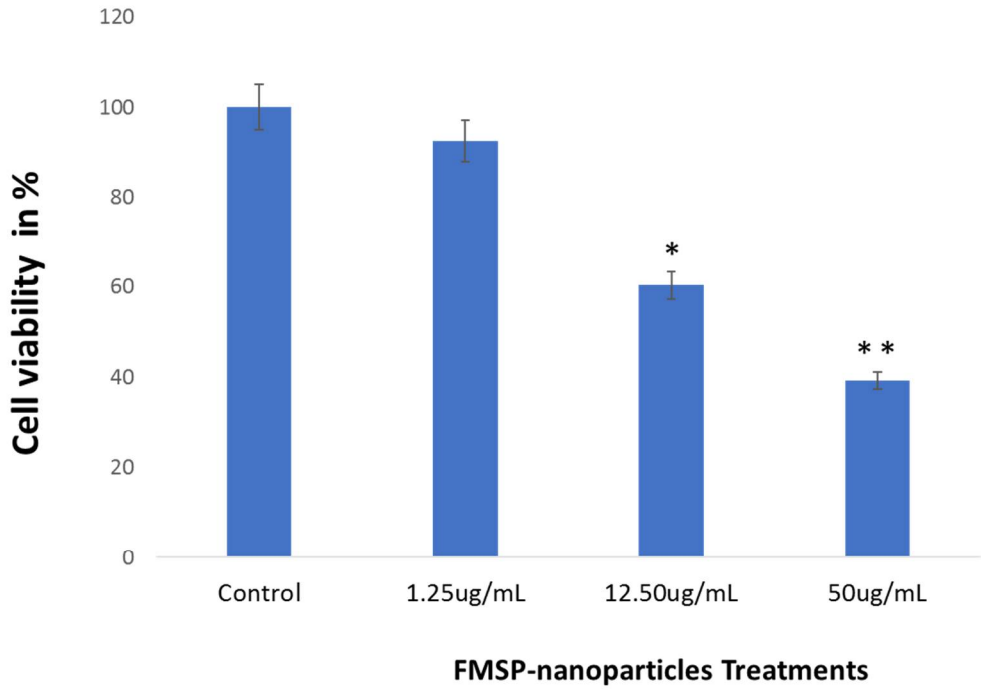


**Cell viability analysis**. The MCF-7 cells were treated with control (no FMSP-nanoparticles treatment) and with different concentrations of FMSP-nanoparticles (1.25 µg/mL , 12.50 µg/mL, and 50 µg/mL) for 24 hrs. Data are the mean ± standard deviation from three replicate measurements. *P < 0.05 and **P < 0.01

## FIGURE LEGENDS

**Figure 1:**

Spherical structure of FMSP-nanoparticles showing through scanning electron microscopy (SEM) with 50,000X magnification.

**Figures 2a-b:**

Structure of FMSP-nanoparticles through transmission electron microscopy (TEM) showing spherical shaped nanoparticles with size ranging from 150 nm to 400 nm.

**Figures 3a-c:**

Cell Morphology: The MCF-7 cells showing morphology (a) Control (nontreated) (b) treated with FMSP-nanoparticles (1.25 µg/mL) for 6hrs (c) treated with FMSP-

nanoparticles (1.25 µg/mL) for 24 hrs: FMSP-nanoparticles-treated cells not showing any morphological changes with compared to control group cells. 100 X magnification

**Figures 4a-c:**

Cell Morphology: The MCF-7 cells showing morphology (a) Control (nontreated) (b) treated with FMSP-nanoparticles (1.25 µg/mL) for 6hrs (c) treated with FMSP-nanoparticles (1.25 µg/mL) for 24 hrs: FMSP-nanoparticles-treated cells not showing any morphological changes with compared to control group cells. 400 X magnification.

**Figures 5a-c:**

Cell Morphology: The MCF-7 cells showing morphology (a) Control (nontreated) (b) treated with FMSP-nanoparticles (12.5 µg/mL) for 6hrs (c) treated with FMSP-nanoparticles (12.5 µg/mL) for 24 hrs: FMSP-nanoparticles-treated cells showing cell death (arrows) after 24hrs of post-FMSP-nanoparticles treatment. 100 X magnification

**Figures 6a-c:**

Cell Morphology: The MCF-7 cells showing morphology (a) Control (nontreated) (b) treated with FMSP-nanoparticles (12.5 µg/mL) for 6hrs showing beginning of cell death (arrows) (c) treated with FMSP-nanoparticles (12.5 µg/mL) for 24 hrs: FMSP-nanoparticles-treated cells showing high level of cell death (arrows) after 24hrs of post-FMSP-nanoparticles treatment. 400 X magnification

**Figures 7a-c:**

Cell Morphology: The MCF-7 cells showing morphology (a) Control (nontreated) (b) treated with FMSP-nanoparticles (12.5 µg/mL) for 6hrs showing high level of cell death (arrows) (c) treated with FMSP-nanoparticles (12.5 µg/mL) for 24 hrs showing

drastic increase in the cell death (arrows) after 24hrs of post-FMSP-nanoparticles treatment. 100 X magnification.

**Figures 8a-c:**

Cell Morphology: The MCF-7 cells showing morphology (a) Control (nontreated) (b) treated with FMSP-nanoparticles (12.5 µg/mL) for 6hrs showing high level of cell death, nuclear disintegration, nuclear augmentation (arrows) (c) treated with FMSP-nanoparticles (12.5 µg/mL) for 24 hrs showing drastic increase in the cell death, nuclear disintegration, nuclear augmentation (arrows) after 24hrs of post-FMSP-nanoparticles treatment. 400 X magnification

**Figures 9a-b:**

Scanning confocal microscopic images of MCF-7 cells stained with DAPI (blue color): The control cells (without FMSP-nanoparticles treatment) (a) and with FMSP-nanoparticles (1.25 µg/mL) (b), 12.5ug/mL (c) and 50ug/mL (d)

**Figure 10:**

Cell viability analysis. The MCF-7 cells were treated with FMSP-nanoparticles with concentrations (1.25 µg/mL, 12.50 µg/mL, and 50 µg/mL) for 24 hrs. Data are the means ± SD of three different experiments. Difference between two treatment groups were analysed by student's t test where (*$p<0.05$), p-values were calculated by Student's t-test.